PHYSICAL REVIEW C VOLUME 17, NUMBER 1 JANUARY 1978

Method for optical model analysis of alpha-nucleus elastic scattering

E. Friedman* and C. J. Batty
Rutherford Laboratory, Chilton, Didcot, Oxon, United Kingdom
(Received 30 June 1977)

A new method for analyzing α-nucleus optical potentials is presented. It consists of adding to the conventional Woods-Saxon real potential an extra potential given by a Fourier-Bessel series. The coefficients of the series are determined by least-squares fit to experimental cross sections for elastic scattering. A detailed discussion of the uncertainties in the derived parameters is presented, both for the real potential as a function of radius and for integral quantities such as the volume integral and the root-mean-square radius. The method is illustrated using existing data over wide angular range for the elastic scattering of 139 MeV α particles by ^{58}Ni and of 104 MeV α by ^{40}Ca, where with the new method χ^2 per degree of freedom is reduced by a factor of between 5 and 7 to a value of almost 1. The method is also used for the analysis of data for 104 MeV α particles scattered by ^{208}Pb, which is restricted to the diffraction region of the angular distribution. In that case the new method is capable of uniquely specifying the region where the real potential is well determined. Evidence is presented for saturation effects in the folding model.

[NUCLEAR REACTIONS α-nucleus optical potentials; modifications to Woods-Saxon form using Fourier-Bessel series. ^{40}Ca(α,α), ^{208}Pb(α,α), E_α=104 MeV. ^{58}Ni(α,α), E_α=139 MeV.]

I. INTRODUCTION

In optical model descriptions of elastic scattering there usually is some residual dependence of the results on the particular choice of parameterized form for the potential. The Woods-Saxon (WS) form has been widely and very successfully used to describe optical potentials for nucleons as well as for composite projectiles. However, this form gives an implicit coupling between the surface region and the interior of the potential and this could introduce undesirable constraints in the analysis. Indeed, in some analyses of very extensive and accurate data,[1,2] the best values of χ^2/F, the χ^2 per degree of freedom, are considerably larger than one indicating possible deficiencies in the form of potentials used. Alternatively, when the data are clearly capable of determining only the surface regions of the nucleus, the WS form leads to estimates of the uncertainty in the potential in the interior of the nucleus which are unrealistically small. Some attempts have been made to improve on the WS form, and it has recently been shown for α particles[3] that better fits to the data could be obtained either by using the square of the WS form for the real part of the optical potential, or by adding to the WS potential an extra term which is centered near the nuclear surface. The use of the square of the WS form has also been suggested in connection with the elastic scattering of heavy ions.[4]

The elastic scattering of α particles provides a good case for studying modifications to the conventional WS description of the optical potential. In this case there are no spin or isospin dependent terms, and therefore it is easier to study the main part of the optical potential. Also, due to the relative strength of the absorptive term for α particles, the surface region and the interior of the nucleus may play different roles, which could be revealed when the constraints imposed by the WS form are removed. Finally, and perhaps most importantly, there is a considerable amount of extensive and accurate experimental data on the elastic scattering of α particles.

The purpose of this paper is to present a new method for studying phenomenologically the real part of the optical potential. This method is capable, in suitable cases, of reducing values of χ^2/F to almost 1, and providing results for the real optical potential which are independent, to a very large extent, of the form chosen for the description of the optical potential. In particular the present method is free of any theoretical prejudice as to the choice of the correction to the WS form. The imaginary potential is, however, left in the conventional WS form. The method is described in Sec. II, where special emphasis is placed on the analysis of the calculated uncertainties in the potential. Integral quantities of interest such as the volume integral and root-mean-square (rms) radius are also discussed. In Sec. III we present results obtained using this method for the analysis of 139 MeV α scattering by ^{58}Ni and 104 MeV α scattering by ^{40}Ca and ^{208}Pb. In Sec. IV we discuss the present results, comment on possible connec-

tions with the folding model, and finally present a summary of some practical points relating to the new method.

II. METHOD

A. Optical potential

Looking for an improvement to the conventional WS form employed in phenomenological descriptions of the real part of the optical potential, we aimed at using a form which was as flexible as possible. The form chosen in the present work consists of a Fourier-Bessel (FB) expansion of part (or the whole) of the real potential, namely,

$$V(r) = -V_0/(e^x+1) - \sum_{n=1}^{N} b_n j_0(q_n r)\,, \qquad (1)$$

where $x=(r-r_0A^{1/3})/a$, and V_0, r_0, and a are the parameters of a best-fit WS potential. $j_0(q_nr)$ are spherical Bessel functions and $q_n=n\pi/R$, where R is a suitably chosen cut-off radius beyond which the extra potential in (1) vanishes, i.e., for $r\geq R$ only the WS form is used. The b_n coefficients are determined by least-squares fit to the experimental results. Similar approaches have been used in the description of charge distributions in nuclei.[5-7] However, there are several differences between the two cases: (i) in the present case the volume integral of the potential is not fixed and therefore there are no constraints imposed on the coefficients b_n. (ii) We do not assume that the extra potential given by the FB series is small, and no linearization of the least-squares-fit equations is attempted. In fact, the method will also work *without* the WS term in (1). However, in this latter case the cut-off of the total optical potential is then an undesirable feature and the least-squares fits become more difficult numerically. The method is then also somewhat analogous to that used by Dreher *et al.*[7] for analyses of elastic scattering of electrons but unlike that case where the coefficients are directly related to the form factor, the b_n coefficients in the present problem have no direct relation to experimentally determined quantities nor to the momentum transfer in the scattering process. They are determined only via the χ^2 fits to the data and the choice of the FB expansion for the optical potential is by no means a "best" choice. In fact, we have obtained very similar results using associated Laguerre polynomials. The FB expansion, however, seems to be more suitable from the numerical analysis point of view and only results for the FB method will be presented here.

The method consists, therefore, of parametrizing the real part of the optical potential by Eq. (1) and using for the imaginary part an independent WS form. An FB series could also be used for the imaginary potential, but it was felt that at present this was not justified and that the real potential should be studied first. Values of R, the cutoff radius for the FB series, are chosen to be well beyond the strong absorption radius,[8] and the number of terms N determined by the fits to the data, i.e., we choose the value of N for which χ^2/F ceases to decrease significantly when N is increased. Values of N between 9 and 11 were found to be adequate, which means that only fairly low Fourier components are determined. As pointed out earlier, N is not directly related to the momentum transfer in the scattering process.

Values of the coefficients b_n in Eq. (1) are determined by a least-squares fit to the data. As a first stage, the six parameters of a conventional complex WS potential are obtained by a standard least-squares fit to the data. In the second stage, we search on the parameters b_n *and* on the three parameters of the imaginary potential, starting with all the b_n values set to zero. This second stage usually requires less computing time than the first stage, provided the data covers a sufficiently wide angular range (see Sec. III). This rapid convergence has been observed in cases where up to 14 parameters have been varied. The improvement in values of χ^2/F achieved at the second stage of the fit can be by almost a factor of 10. The method is found to be very flexible in providing modifications to the WS form, but its main advantage is, perhaps, in providing estimates of uncertainties in the potential which we discuss next.

B. Uncertainties in the potential

In the course of calculating the parameters of the potential by least-squares fits to experimental results the uncertainties in the parameters are usually determined from the diagonal elements of the covariance matrix. (See below.) However, the uncertainties in the best-fit parameters are not sufficient for the evaluation of uncertainties in quantities of interest and one also needs to know the correlations between the various parameters. For example, suppose the least-squares fit to the data determines the FB coefficients to accuracies $\pm\Delta b_n$. Then the mean square uncertainty in the value of the potential at a radius r is given by

$$[\Delta V(r)]^2 = \sum_{m,n=1}^{N} \langle \Delta b_m \Delta b_n \rangle_{\rm av} j_0(q_m r) j_0(q_n r) \qquad (2)$$

and the correlations between the coefficients, $\langle \Delta b_m \Delta b_n \rangle_{\rm av}$, are required. [Note that the WS potential in (1) does not enter here because it essentially serves to determine the initial values for the FB fit]. The correlations are found to be very important in the present problem and this is another

essential difference when compared with the electron scattering case.

The general result for the correlations between the different parameters obtained in least-squares fits is a well-known one readily derived by standard methods of matrix algebra. Writing χ^2/F as a function of some parameters a_n

$$\chi^2/F = f(a_1 \cdots a_L) \tag{3}$$

a matrix M is formed from the partial derivatives of f at a minimum of f, namely,

$$M_{mn} = \left(\frac{\partial^2 f}{\partial a_m \partial a_n}\right)_{\min} . \tag{4}$$

Diagonalization of the positive definite symmetric matrix M leads to

$$\langle \Delta a_m \Delta a_n \rangle_{\rm av} = (M^{-1})_{mn} f_{\min} , \tag{5}$$

where $f_{\min}$ is the value of χ^2/F at a minimum and M^{-1} is usually referred to as the covariance matrix. If $f_{\min}$ is significantly greater than one then the uncertainties lose their statistical meaning. The uncertainty in the derived real part of the optical potential as a function of r is therefore given by

$$\Delta V(r) = \left[f_{\min} \sum_{m,n=1}^{N} (M^{-1})_{mn} j_0(q_m r) j_0(q_n r) \right]^{1/2} . \tag{6}$$

The volume integral (J) and rms radius of the real part of the optical potential ($\langle r^2 \rangle^{1/2}$) are quantities of interest, mainly in connection with the "microscopic" aspects of the potential.[9] Writing $J = J_0 + J_1$, where J_0 is the volume integral of the WS component in (1), J_1 is given by the FB coefficients as follows

$$-J_1 = \frac{4R^3}{\pi} \sum_{n=1}^{N} \frac{(-1)^{n+1}}{n^2} b_n \tag{7}$$

and the uncertainty is given by

$$\Delta J = \frac{4R^3}{\pi} \left[f_{\min} \sum_{m,n=1}^{N} \frac{(-1)^{m+n}}{m^2 n^2} (M^{-1})_{mn} \right]^{1/2} . \tag{8}$$

Similarly, the rms radius and its uncertainty can be obtained from $\langle r^2 \rangle J = \langle r_0^2 \rangle J_0 + \langle r_1^2 \rangle J_1$ (in obvious notation) using the following expressions

$$-\langle r_1^2 \rangle J_1 = \frac{4R^5}{\pi^3} \sum_{n=1}^{N} \frac{(-1)^{n+1}}{n^4} (\pi^2 n^2 - 6) b_n \tag{9}$$

and

$$\Delta(\langle r^2 \rangle J) = \frac{4R^5}{\pi^3} \left[f_{\min} \sum_{m,n=1}^{N} \frac{(-1)^{m+n}}{m^4 n^4} \times (\pi^2 m^2 - 6)(\pi^2 n^2 - 6)(M^{-1})_{mn} \right]^{1/2} . \tag{10}$$

In the next section the particular features of the present method are demonstrated by analyses of several sets of experimental results.

III. RESULTS

Three sets of experimental results have been used to illustrate the power of the present method. The first[10] is for the elastic scattering of 139 MeV α particles by ^{58}Ni. This is the same data which enabled Goldberg and Smith[11] to eliminate the so-called discrete ambiguity in the real optical potential. The second[12] is for the elastic scattering of 104 MeV α particles by ^{40}Ca. This angular distribution consists of 112 data points and extends to large angles. These results are also analyzed over two different angular ranges in order to assess the relevance of the "rainbow angle" criteria of Goldberg *et al.*[2,10,11] to the present method. The third set of experimental results[13] is for the elastic scattering of 104 MeV α particles by ^{208}Pb, where the angular distribution is restricted to the diffraction region.

A. ^{58}Ni(α,α) at 139 MeV

This set of experimental results[10] consists of 50 differential cross sections measured between 8° and 79°. As the present method uses 10–14 parameters to describe the optical potential, only the full angular range was analyzed. Results of the least-squares fits are given in Table I. The present results for the WS model differ slightly from those of Ref. 10 probably due to the inclusion of relativistic effects[14] in the present work. The

TABLE I. Results of optical model fits to ^{58}Ni(α,α) at 139 MeV. Errors are quoted only for the present Fourier-Bessel method. J is the volume integral and $\langle r^2 \rangle^{1/2}$ is the rms radius of the real optical potential.

Model	χ^2/F	$-J/4A$ (MeV fm^3/nucleon pair)	$\langle r^2 \rangle^{1/2}$ (fm)
Woods-Saxon	6.2	290	4.74
Woods-Saxon plus 11 FB terms ($R = 13$ fm)	1.2	281 ± 3	4.69 ± 0.07

second stage of the fit, namely, fitting the coefficients b_n in (1) (and readjusting the imaginary potential) converged very rapidly and produced a significant reduction in the value of χ^2/F. The parameters for the imaginary potential changed very little in this stage of the search. Figure 1 shows the real potential obtained for the best-fit WS form as well as for the best-fit WS plus 11 terms for the FB series. An interesting feature is the variation of the estimated uncertainties with r. The potential is rather poorly determined at the nuclear center, but quickly becomes well determined as r increases; such a result is clearly impossible to get using a WS parametrization (even when correlations are included in the analysis of uncertainties). The accuracy is reduced at large radii, but this is not observed in Fig. 1. (See, however, Fig. 4). Note that the uncertainties displayed in Fig. 1 are not uncorrelated, and generally $\langle \Delta V(r)\Delta V(r') \rangle_{av} \neq 0$. These correlations are however automatically included when the uncertainties in J and $\langle r^2 \rangle^{1/2}$ are calculated.

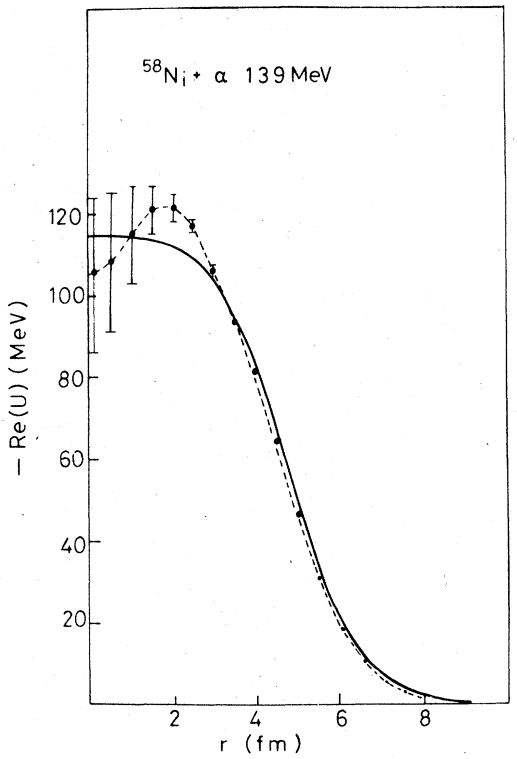

FIG. 1. Real part of optical potential for ^{58}Ni(α,α) at 139 MeV, for conventional WS model (continuous curve) and for the present method, with 11 FB terms, $R = 13$ fm (dashed curve). Note that the errors are not uncorrelated.

B. ^{40}Ca(α,α) at 104 MeV

Results of optical model fits to the full range of the angular distribution, which consists of 112 points between 5° and 116°, are given in the first part of Table II, and the fit to the data obtained using the present method is shown in Fig. 2. As in the case of ^{58}Ni, convergence of the second stage of the least-squares search was rapid, and as can be seen from Table II and Fig. 2, the fit to the data is very good. Again, the parameters of the imaginary potential changed very little in the second stage of the search. Figure 3 shows the real part of the optical potential for the WS model and for the WS plus 11 FB terms. Compared to ^{58}Ni, it is seen that the uncertainties in the potential are smaller and it looks as if for these ^{40}Ca

TABLE II. Results of optical model fits to ^{40}Ca(α,α) at 104 MeV. Errors are quoted only for the present Fourier-Bessel method. J is the volume integral and $\langle r^2 \rangle^{1/2}$ is the rms radius of the real optical potential.

Angular range	Model	χ^2/F	$-J/4A$ (MeV fm^3/nucleon pair)	$\langle r^2 \rangle^{1/2}$ (fm)
5°–116°	Woods-Saxon	10.5	332	4.45
	Woods-Saxon plus 11 FB terms ($R = 13$ fm)	1.5	323 ± 2	4.36 ± 0.04
5°–48°	Woods-Saxon	2.8	339	4.37
	Folding	1.8	393	4.09
	Woods-Saxon plus 11 FB terms [a] ($R = 13$ fm)	0.9	296 ± 10	4.33 ± 0.17
22°–116°	Woods-Saxon	12.3	335	4.47
	Woods-Saxon plus 11 FB terms ($R = 13$ fm)	1.8	333 ± 16	4.5 ± 0.5

[a] An example of a typical, but not unique result.

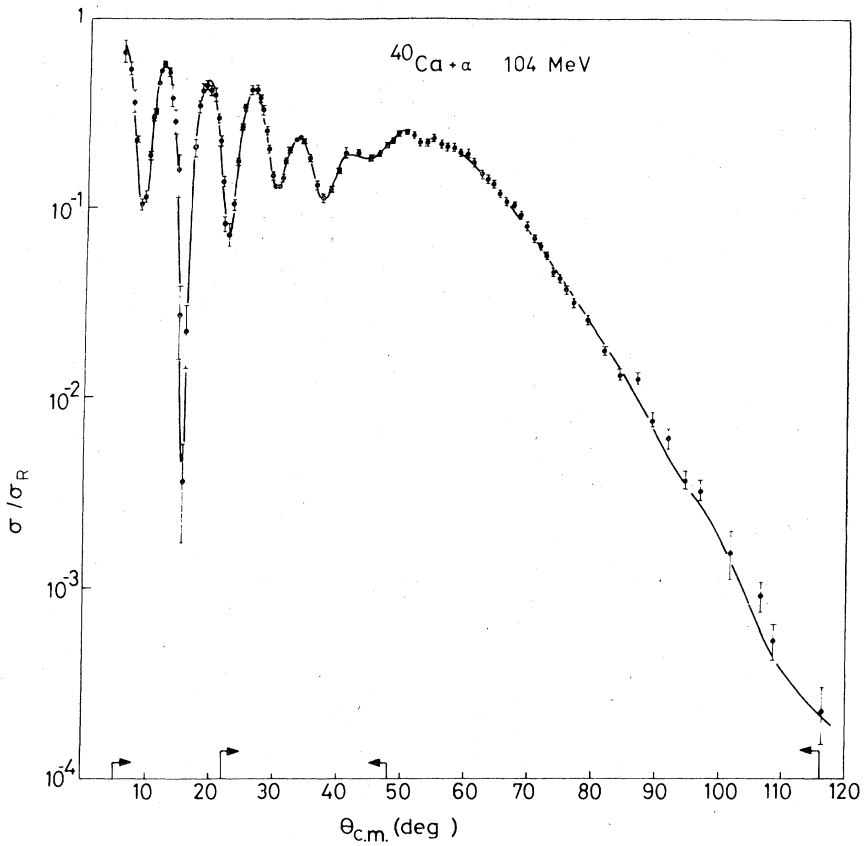

FIG. 2. Experimental angular distribution for ^{40}Ca(α, α) at 104 MeV (Ref. 12) and calculated best-fit angular distribution obtained by the present method. (Several experimental points for angles smaller than 10° have been omitted from the figure for clarity). Two angular ranges used in separate fits are indicated by arrows.

data that the α-particle probes the interior of the nucleus more completely.

Separate optical model fits have been made to the experimental results using the 73 data points between 5° and 48°. This range is in the diffraction region of the angular distribution, and according to the criteria of Goldberg *et al.*[10,11] the data over this range are incapable of providing a unique real optical potential in the nuclear interior. The results of the present work are in agreement with this conclusion. The second part of Table II shows that a reasonably good fit is obtained with the WS form and some improvement is obtained when the FB series is included. However, the second stage of the parameter search took a very long time to converge (unlike the previous case where the large angle data were included), and it was possible to obtain convergence to different sets of parameters, which were not always consistent with each other. In particular, values of the volume integral did not always agree and the discrepancies were larger than the estimated uncertainties. This indicates that the present method is of limited use when the data are restricted to relatively small angles, or put in other words, when the data are not extensive enough[15] to enable information to be obtained about the nuclear interior.

The elastic scattering of α particles by ^{40}Ca in the diffraction region has been used[9,13] to "calibrate" the effective α-nucleon interaction for the folding model. We have also used the folding model for this angular region and in Table II are shown results assuming identical neutron and proton densities[16] (with rms radius of 3.39 fm) and searching on the α-nucleon interaction and the imaginary potential. The fit is quite good, probably because under these conditions of restricted data, the extra constraints imposed on the potential via the folding model are useful.[14] The α-nucleon interaction obtained in this fit is very reasonable. Values of $-J/4A$ of 393 MeV fm^3 and rms radius of the interaction of 2.29 fm (obtained from the rms radii of the potential and of the matter distribution) are in excellent agreement with previous determinations[9,13] of these quantities. Very recently Lassut and Vinh Mau[17] obtained parameters for the effec-

tive α-nucleon interaction, starting from the nucleon-nucleon interaction. At 104 MeV they obtain $-J/4A$ in the range 317 to 400 MeV fm^3 and rms radii in the range 2.1 to 2.4 fm. Our empirical results clearly agree with these values.

If the results for $-J/4A$ and $\langle r^2 \rangle^{1/2}$ obtained in the present work from the fit over the *full* angular range (see first part of Table II) are to be interpreted in terms of a simple folding model, then the effective interaction should have an rms radius of 2.74 fm. The apparent reduction of $-J/4A$ from 393 to 323 MeV fm^3 which is accompanied by an increase in the rms radius of the interaction from 2.29 to 2.74 fm when the large angle data are included indicates saturation of the interaction as the penetration into the nucleus becomes deeper, a result which is to be expected. This means that large angle data cannot be analyzed with the simple folding model using a density-independent interaction. We return to this point in Sec. IV.

Optical model fits have also been made to that part of the data which only covered larger angles. The third part of Table II gives results for the 73 data points in the range of 22° to 116°. Here the second stage of the parameter search converged very quickly to a well-defined result. The real part of the optical potential agrees very well with the potential obtained by fits to the full angular range. Several points near the center of the nucleus obtained for the large-angle fit are included in Fig. 3. For $r \geq 1.5$ fm the two potentials are indistinguishable on the scale of Fig. 3. However, the results for the volume integral and the rms radius show significant differences between the partial and full angular ranges. Comparing the first and third parts of Table II, we see that the corresponding results agree, within their estimated uncertainties but the exclusion of the data below 22° causes an 8-fold increase in the uncertainty in the volume integral and a 12-fold increase in the uncertainty in the rms radius. This is undoubtedly due to the fact that the small angle data are sensitive mainly to interactions at large radii. This result provides an interesting demonstration of the power of the present method and in particular of the analysis of the uncertainties.

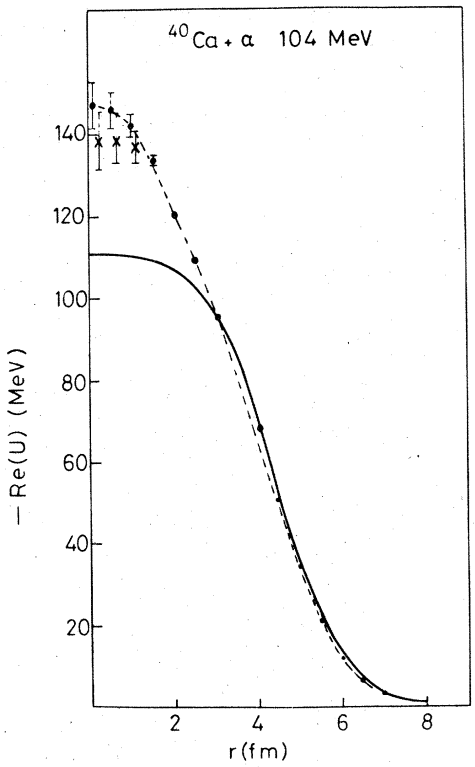

FIG. 3. Real part of optical potential for ^{40}Ca(α, α) at 104 MeV for conventional WS model (continuous curve) and for the present method, with 11 FB terms, $R = 13$ fm (dashed curve). Also shown are several points (crosses) for the fit obtained for the 22°–116° data.

C. ^{208}Pb(α,α) at 104 MeV

In this case[13] the data are well within the diffraction region of the angular distribution and therefore there is little hope of extracting any information about the nuclear interior.[14] Under these circumstances one cannot expect to get a unique description of the optical potential. Calculations using the present method took a very long time to converge and lead generally to nonunique results. However, a region of the potential near the strong absorption radius was found to be very well determined. This is, of course, a well known result, but an interesting feature of the present method is that indeed the uncertainties are predicted to be very small in that region. Examples for two such fits are shown in Fig. 4 where it is clearly seen that the uncertainties are very small near $r = 10$ fm. The folding model appears to be more suitable for analyzing small-angle data but, nevertheless, the present method shows which are the well determined regions of the potential.

IV. DISCUSSION

A. General

A new method for analyzing phenomenologically the real part of the α-nucleus optical potential has been developed. The method consists of adding to the conventional WS potential an extra potential given by a Fourier-Bessel series, where the coefficients are determined by a least-squares fit to the data. In the examples shown here values of χ^2/F decreased by factors of between 5 and 7 to val-

ues close to 1. Although the number of parameters has increased from 6 in the conventional model to up to 14 in the new method, this is still a small number compared with typically 50 to 100 experimental data points in a good angular distribution. The present method is free from any prejudice as to the form of the modification to the WS parametrization and the analysis of the uncertainties in the potential is particularly powerful. The method is at its best when the data extend well beyond the nuclear "rainbow angle,"[2] i.e., well beyond the diffraction region of the angular distribution into the region of exponential decrease. In such cases the convergence of the parameter search is very rapid and a single calculation is capable, thanks to the estimated uncertainties, of showing clearly the regions of the potential which are well determined. This is in contrast to the approach[18] of introducing a local perturbation into the WS potential and repeating the least-squares fits many times, varying the location of the perturbation in order to ascertain which are the well-determined regions of the potential. The alternative method of Brissaud and Brussel[19] using a sum of Gaussians to describe the matter distribution is essentially a folding method, but again involves 10's of repeats of the least-squares-fitting procedure. This last method could have advantages for analyses of data over a restricted angular range.

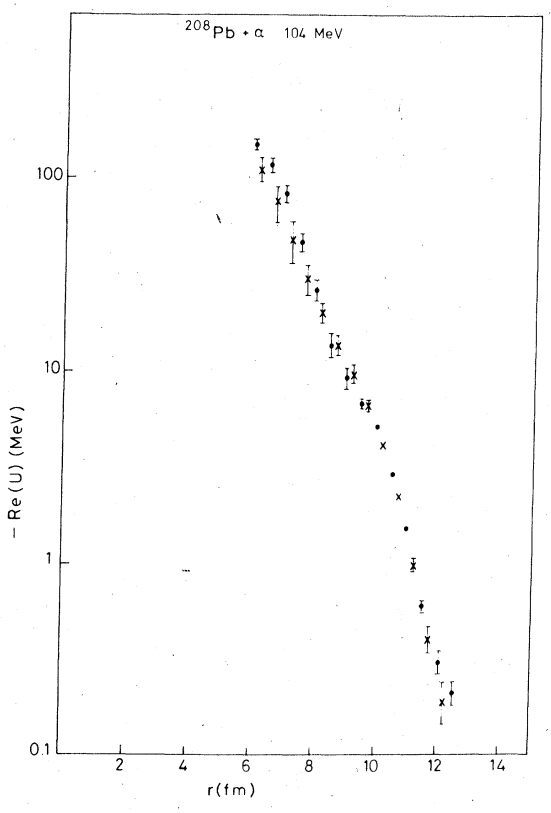

FIG. 4. Real part of optical potential for ^{208}Pb(α, α) at 104 MeV. Dots and crosses indicate two different fits to the data.

The present method is not very efficient when the data do not include cross sections for sufficiently large angles. This is not a deficiency of the method but it is more clearly observed here than in the simple WS parametrization where coupling between the surface region and the interior is implicit in the model. In situations where the data do not probe the nuclear interior, the extra flexibility available in the present method is not justified although it can still clearly indicate the region near the surface where the potential is well determined.

We have stressed the importance of experimental results for large angles, but the role of experimental results at small angles should not be overlooked. That has been clearly demonstrated by the uncertainties in the values of the volume integral and rms radius in the analysis of the results for ^{40}Ca.

The present method is, obviously, not "model independent." The cutoff radius R and the number of terms N cannot be varied, in practice, beyond reasonable limits and there is some dependence on the initial values provided by the best-fit WS potential. For example, starting the second stage of the search for ^{58}Ni with $\chi^2/F = 1600$ (compared to 6.2 in the best fit), the final χ^2/F was 3 (compared to 1.2) and the potentials did not agree for $r \leq 2.5$ fm, probably due to the value of N being too small in this case. Nevertheless, values of J and $\langle r^2 \rangle^{1/2}$ agreed within their estimated uncertainties. Starting from any reasonable WS fit, the searches converge quickly to produce a well defined potential. The dependence of the results on the form chosen for the potential is considerably smaller in the present method than in conventional analyses. We also note that the imaginary potential used here is of the traditional WS form and this could have a small effect on the results.

Finally, the present method may be suitable for analyses of heavy-ion scattering, where it could help settle the question of whether the optical potential at small separations can be determined.[20]

B. Relationship to more fundamental models

The description of the scattering process in terms of a local phenomenological potential is a very useful approximation. More fundamental approaches which are based on nucleon-nucleon interactions and which may involve, for example, exchange effects, are seldom employed in direct comparisons with extensive experimental results.

Instead, the resulting interaction can be approximated by a local and energy-dependent optical potential, and the latter compared with the results of phenomenological analyses.[21] Such comparisons however, may not be very meaningful when the details of the phenomenological potential itself may depend on the particular choice of parametrization and when values of χ^2/F are significantly greater than 1. The present method offers an improvement to phenomenological optical potentials which may be used as an intermediary in confronting more fundamental theories with experiments.

A particularly simple form of a more fundamental approach is provided by the folding model[9] which has been used in direct comparisons with experimental data. In the analysis of the ^{40}Ca data we indicated possible difficulties in relating the results of the present method to the simple folding model. These difficulties are observed when comparing results obtained from fits over the full angular range with those obtained from fits over the diffraction region only. In the former case the volume integral and rms radius of the real potential are well determined but in the latter there are ambiguities and we choose, for a comparison, the folding model fit which leads to unambiguous results and acceptable value of χ^2/F. The values obtained for the volume integrals and rms radii suggest saturation effects as the probing of the nucleus becomes deeper, hence making questionable the merit of analyzing *large angle* data with the simple folding model. However, using a simple Gaussian in the folding model, one could be tempted to *technically* take advantage of the Fourier-Bessel series in the present method and unfold analytically an effective α-N interaction in order to obtain a nuclear matter density distribution. We wish to discourage such an approach.

As mentioned in Sec. II, an FB expansion of the potential is possible also without the WS term in (1). (The initial values of b_n are then taken from a Fourier-Bessel expansion of the best-fit WS.) In that case, unfolding a Gaussian with a range parameter μ leads to FB coefficients for the nuclear matter distribution $b_n^{(m)}$ as follows

$$b_n^{(m)} = \frac{A}{-J}\, b_n \exp\left[\left(\frac{\pi\mu}{2R}\right)^2 n^2\right] \tag{11}$$

and the covariance matrix can also be transformed into the matter distribution. Because of the finite cutoff radius R, Eq. (11) is expected to hold only for small values of n even for folding calculations. Also, it is well known that unfolding procedures are quite often unreliable because of propagation of errors. We have verified that the present case is no exception. Applying (11) to the b_n coefficients obtained for ^{40}Ca from fits over the full angular range produced results which were numerically meaningless. It is felt, however, that these observations are worth reporting.

C. Practical comments

As demonstrated in the present work, the new method is particularly useful in cases when the data contain cross sections for angles beyond the diffraction region. The most efficient approach is to first fit a WS potential and only then perform the least-squares fit for the FB series, together with further adjustments of the imaginary potential. A search then over for example 14 variables does not require more computing time than the conventional WS fit. Typical values for R, the cutoff radius are 13–16 fm and about 10 terms in the series were found to be sufficient. Failure to converge in a reasonably short computing time usually indicates either too stringent convergence criteria or that the data are incapable of providing a reasonably well determined optical potential throughout the nuclear volume. In such cases the uncertainties in the potential as given by the present method could be underestimates, particularly close to the center. Results for volume integrals and rms radii are, however, usually reliable.

---

*Permanent address: The Racah Institute of Physics, The Hebrew University, Jerusalem, Israel.

[1]G. Hauser, R. Löhken, H. Rebel, G. Schatz, G. H. Schweimer, and J. Specht, Nucl. Phys. A128, 81 (1969).

[2]D. A. Goldberg, S. M. Smith, and G. F. Burdzik, Phys. Rev. C 10, 1362 (1974).

[3]D. A. Goldberg, Phys. Lett. 55B, 59 (1975); N. S. Wall, A. S. Cowley, R. C. Johnson, and A. M. Kobos (unpublished).

[4]L. D. Rickertsen and G. R. Satchler, Phys. Lett. 66B, 9 (1977).

[5]U. Meyer- Berkhout, K. W. Ford, and A. E. S. Green, Ann. Phys. (N.Y.) 8, 119 (1959).

[6]J. L. Friar and J. W. Negele, Nucl. Phys. A212, 93 (1973).

[7]B. Dreher, J. Friedrich, K. Merle, H. Rothhaas, and G. Lührs, Nucl. Phys. A235, 219 (1974).

[8]B. Fernandez and J. S. Blair, Phys. Rev. C 1, 523 (1970).

[9]A. M. Bernstein and W. A. Seidler, Phys. Lett. 34B, 569 (1971).

[10]D. A. Goldberg, S. M. Smith, H. G. Pugh, P. G. Roos, and N. S. Wall, Phys. Rev. C 7, 1938 (1973).

[11]D. A. Goldberg and S. M. Smith, Phys. Rev. Lett. 29, 500 (1972).
[12]D. Habs, G. Hauser, G. Hoffmann, H. Klewe-Nebenius, R. Löhken, U. Martens, H. Rebel, G. Schatz, G. W. Schweimer, and J. Specht, Kernforschungszentrum Karlsruhe Report No. 18/70-2, 1970 (unpublished).
[13]H. J. Gils and H. Rebel, Phys. Rev. C 13, 2159 (1976); H. J. Gils, H. Rebel, J. Buschmann, H. Klewe-Nebenius, G. P. Nowicki, and W. Nowatzke, Z. Phys. A279, 55 (1976).
[14]E. Friedman and C. J. Batty, Phys. Rev. C (to be published).
[15]P. P. Singh and P. Schwandt, Phys. Lett. 42B, 181 (1972).
[16]C. W. de Jager, H. de Vries, and C. de Vries, At. Data Nucl. Data Tables 14, 479 (1974).
[17]M. Lassaut and N. Vinh Mau (private communication).
[18]D. G. Madland, P. Schwandt, W. T. Sloan, P. Shapiro, and P. P. Singh, Phys. Rev. C 9, 1002 (1974); P. J. Moffa, C. B. Dover, and J. P. Vary, *ibid.* 13, 147 (1976).
[19]I. Brissaud and M. K. Brussel, J. Phys. G 3, 481 (1977).
[20]G. R. Satchler, Nucl. Phys. A279, 493 (1977).
[21]J.-P. Jeukenne, A. Lejeune, and C. Mahaux, Phys. Rev. C 16, 80 (1977).